Fluorescence in Mg IX emission at 48.340 Å from Mg pinch plasmas photopumped by Al XI line radiation at 48.338 Å

N. Qi,* D. A. Hammer, D. H. Kalantar, and K. C. Mittal
Laboratory of Plasma Studies, Cornell University, Ithaca, New York 14853
(Received 30 August 1991; revised manuscript received 8 September 1992)

Resonant photopumping of Be-like Mg IX ions by Li-like Al XI line radiation has been studied in pulsed-power-driven plasmas as a possible approach to achieve laser action in the extreme-ultraviolet wavelength region. An Al x-pinch or z-pinch plasma imploded by a 0.5-TW pulsed power generator produced intense line radiation at 48.338 Å. A separate Mg z-pinch plasma, driven by the same pulsed power generator, was created in parallel with 1 cm separating the two plasmas. Evidence for fluorescence (resonant scattering) was the appearance of 48.340-Å resonance line emission from the 4p level of Mg IX ions due to photopumping by the Al XI line radiation at 48.338 Å. Fluorescence may also have been observed on the Mg VIII line at 52.395 Å, photopumped by Al XI line radiation at 52.446 Å. Both Al and Mg plasmas were characterized in the experiments. Improvements to the pump geometry required to achieve gain on the Mg IX line at 228 Å are also discussed.

I. INTRODUCTION

The development of a compact, low-cost extreme ultraviolet (xuv) or soft-x-ray laser system will almost certainly lead to its use as a laboratory tool by scientists in biology, biophysics, crystallography, solid-state physics, etc. [1]. The recent successful achievement of xuv lasers powered by laser drivers in experiments at Lawrence Livermore National Laboratory [2] (LLNL) and Princeton Plasma Physics Laboratory [3] (PPPL) represents a very important step forward toward the achievement of the desired laboratory tool. However, major technological advances are still needed to avoid requiring large, expensive laser systems and large staffs of technicians and/or scientists in order to make an xuv or x-ray laser. While it is certainly possible that compact, low-cost, easily operated laser systems can be developed to power useful xuv or soft-x-ray lasers [4,5] as demonstrated by the gain measurements at PPPL [6], an attractive alternative power source for such lasers is the pulsed power generator [7]. Pulsed power is potentially more efficient than lasers at powering a laser medium, is less costly on a per-joule basis, and pulsers with energies greater than the state-of-the-art Nova laser facility (at LLNL) [2] are available now in several laboratories. All of this translates into the *possibility* of a relatively low-cost, compact xuv or soft-x-ray laser using state-of-the-art pulsed power techniques *if* laser action can be demonstrated. Specifically, a 10^{12}-W pulser capable of delivering $\gtrsim 1$ MA to a load in a ~ 100-ns pulse on a low repetition rate basis (e.g., one pulse per hour) for xuv laser experiments can probably be built for under \$1 million using state-of-the-art techniques, and would take up less than 200 ft^2 of floor space, including its power supplies.

Pulsed power also has a major disadvantage relative to lasers for serving as an xuv or soft-x-ray laser driver, namely, it is limited to delivering energy to the laser medium on the few-nanosecond time scale or greater, rather than the ≤ 2-ns time scale used so successfully in the LLNL xuv laser program. Thus, population inversion through collisional excitation requiring a uniform lasing medium with an electron density $\gg 10^{20}$ cm^{-3} and temperature ~ 1 keV, both obtained by laser pumping, are unlikely to be achieved with pulsed power. However, a quasi-cw photoexcitation mechanism, in which the lasing plasma conditions are reduced to an electron density of $\sim 10^{18}$ cm^{-3} and a temperature of tens of electron volts, and a recombination scheme, in which the plasma is cooled by heat conduction to a wall [8,9], are certainly accessible to pulsed power drivers.

The first resonantly photopumped approach to xuv lasers was the NaX–Ne IX scheme. The possibility of laser action on the $n = 4$ to $n = 3$ transition at 230 Å and/or on the $n = 4$ to $n = 2$ transition at 58 Å in He-like Ne ions pumped by H-like Na resonant line radiation at 11 Å was proposed by Vinogradov, Sobelman, and Yukov [10], and later analyzed in detail by Hagelstein [11] and the group at the Naval Research Laboratory (NRL) [12,13]. Experiments using a pulsed power generator were initiated at NRL [14], Sandia National Laboratories (SNLA) [15], and Physics International–Olin [16] to study the Na-Ne scheme, and fluorescence has been demonstrated recently at NRL [17] and SNLA [18]. It is possible that gain at 230 Å in Ne IX can be achieved, which is shorter in wavelength than the observed laser action at 326.5 Å in a laser-produced Ti plasma [19], which is believed to have been pumped by resonant photoexcitation.

The xuv laser concept under investigation here is that discussed by Krishnan and Trebes [20]. They proposed a resonant photopumped scheme in the Be-like isoelectronic sequence, in which lasing is expected on the $2s4p$-$2s3d$ and $2s4f$-$2s3d$ transitions from 2177 Å ($4p$-$3d$) and 2163 Å ($4f$-$3d$) wavelength in C III ions pumped by Mn VI line radiation down to 241 Å ($4p$-$3d$) and 228 Å ($4f$-$3d$) in Mg IX pumped by Al XI line radiation. Lasing at 2177 and 2163 Å from C III ions pumped by the Mn VI resonant line radiation at 310 Å has been demonstrated [21].
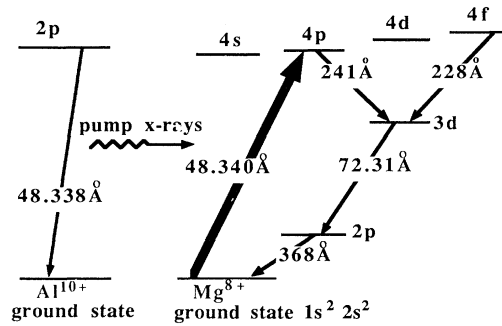
FIG. 1. Simplified energy-level diagram for the Al XI–Mg IX resonant photopumped xuv laser scheme.

To push the lasing wavelength an order of magnitude shorter, it is of interest to investigate the use of the Al XI $1s^2 2s$-$1s^2 2p$ resonance transition at 48.338 Å to pump Mg IX ions leading to possible stimulated emission on the $2s4p$-$2s3d$ transition at 241 Å and on the $2s4f$-$2s3d$ transition at 228 Å. Figure 1 illustrates the principle of the Al XI–Mg IX photopumped xuv laser scheme. Intense Al XI line radiation at 48.338 Å pumps nearby Mg IX ions from the $2s^2\ ^1S$ ground state to the upper $2s4p\ ^1P^\circ$ level. The $2s4p$-$2s^2$ transition in Mg IX is at 48.340 Å. The 2-mÅ wavelength mismatch between the pump and the absorption lines is overcome by the Doppler width of the Al XI pump line. At appropriate electron density and temperature, collisions rapidly transfer the enhanced $4p$ level population to other $n=4$ levels. Resonant photoexcitation of Mg IX ions is expected with enhanced emission from the $n=4$ to $n=2$ and 3 transitions in Mg IX. To achieve population inversion between the levels $n=4$ and $n=3$, the Al pump plasma must be hotter and much more dense ($T_e \sim 150$ eV, $n_e \geq 10^{20}$ cm^{-3}) than the Mg plasma ($T_e \sim$ few tens of eV, $n_e \leq 10^{18}$ cm^{-3}), making spatial separation of the two plasmas a requirement in experiments.

The enhanced emission from the $n=4$ level to the ground state induced by photopumping should be referred to as "resonant scattering" or "resonance radiation." However, in this paper we will follow the common practice of referring to it as fluorescence, along with other enhanced line emissions due to the photopumping.

In this paper, we report the results of fluorescence experiments on the Al XI–Mg IX photopumped laser concept using the 0.5-TW LION (light-ion) pulsed power generator [22]. This work represents the first step toward demonstrating the feasibility of achieving laser action in the xuv from the Al XI–Mg IX scheme. The collisional-radiative kinetics elucidated by these experiments shed light on possible photopumped xuv lasers. The rest of this paper is organized as follows. Section II describes the experimental arrangement. Section III presents the results and discussion of the experiments. In Sec. IV, conclusions from the experiments are presented and future experiments are suggested.

II. EXPERIMENTAL ARRANGEMENT

Figure 2 shows a schematic diagram of the experimental setup. The Al and Mg plasmas were produced in
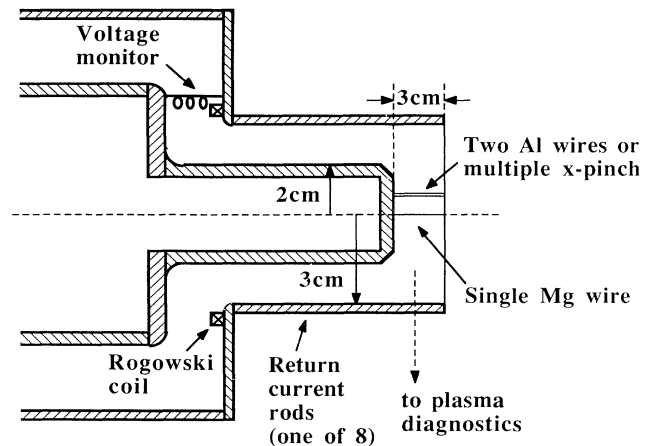

FIG. 2. Schematic diagram of the experimental apparatus showing an example wire load.

parallel or in series by the LION generator with a 30-ns rise time, 80 ns [full width at half maximum (FWHM)], and 400-kA peak current pulse. The 4-cm diameter anode was surrounded by eight 1-cm diameter return current rods on a 6-cm inner diameter circle. The gap between the anode and the cathode was about 3.5 cm.

To produce Al and Mg plasmas separated in space, several specific Al and Mg z-pinch and x-pinch [23,24] load configurations were tested, three of which are shown in Fig. 3. In the configurations shown in Figs. 3(a) and
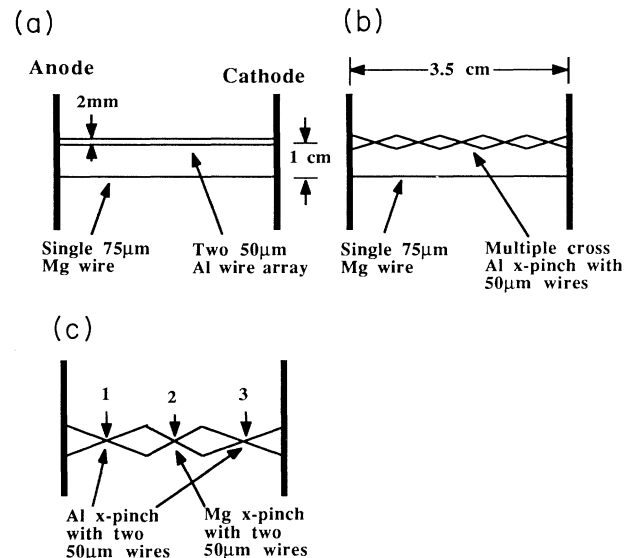

FIG. 3. Specific load configurations A, B, and C used to achieve fluorescence. In configurations A and B, a Mg plasma was produced from a single 75-μm-diam Mg wire on the LION axis. In configuration A, an Al plasma was created from two parallel 50-μm-diam Al wires separated by 0.2 cm and both located 1 cm from the Mg wire. In configuration B, the Al plasma was initiated from two 50-μm-diam Al wires, which were twisted so as to cross at several points. In configuration C, alternating Al and Mg wires crossed such that a Mg plasma was produced from the x-pinch point 2 and Al plasmas were produced at the x-pinch points 1 and 3.

3(b), the Mg plasma was created from a single 75-μm diameter Mg wire located along the electrode axis. In Fig. 3(a), the Al plasma was generated from two 50-μm diameter Al wires placed parallel to each other 0.2 cm apart and both 1 cm from the Mg wire ("configuration A"). In "configuration B", the Al plasma was a multiple cross x pinch made from 50-μm diameter Al wires [Fig. 3(b)], also 1 cm away from the Mg wire. Figure 3(c) shows a three cross x-pinch load configuration ("configuration C"). A Mg plasma was produced at the cross point 2, where two 50-μm Mg wires were twisted and touching, whereas an Al plasma was produced at cross points 1 and 3, where two 50-μm Al wires were crossed. The Al cross points were about 0.5 cm from the Mg cross point. In all cases, the first few nanoseconds of the LION power pulse vaporized the wires and turned them into expanding plasmas. In the case of a single wire, or at the crossing point of an x pinch, the rising current produced self-magnetic pinch forces on the plasma, which stopped the expansion and imploded it back down to small radius. The directed kinetic energy of the implosion then rapidly thermalized, generating a highly ionized, dense, radiating plasma. With parallel wires separated by a few millimeters or less, the individual wire plasmas were attracted toward each other and joined to form a single imploding plasma. It was determined experimentally that a 1-cm separation between the on-axis Mg wire and a parallel wire, wire array, or multiple x pinch would give negligible motion of the Mg plasma toward the other one during the LION power pulse.

Various diagnostics were employed to detect radiation emission. To characterize the emission region geometry, an x-ray pinhole camera was used, in which L-shell radiation with photon energy between 160 (77 Å) and 280 eV (44 Å) and K-shell radiation with photon energy greater than 1240 eV (10 Å) passed through a 4-μm mylar and 1000-Å Al filter and was recorded on Kodak Exploration GWL film. The plasma dynamics during the current pulse were studied by using a visible-light streak camera. The time integrated K-shell (Al and Mg ions) and L-shell (Mg ions) line radiations were measured by a calibrated potassium acid phthalate (KAP) curved crystal spectrograph [25] and by a 1-m grazing incidence spectrograph, respectively. L-shell xuv radiation and K-shell soft x rays were detected by filtered Al cathode x-ray diodes (XRD's), which recorded photons with energy less than 1 keV, and by filtered photoconducting diodes [26] (PCD's), which recorded photons with energy greater than 1 keV, respectively. The diagnostics viewed the plasmas from the radial direction.

III. RESULTS AND DISCUSSION

A. Evidence for fluorescence, configurations A and B

By suitable choice of wire mass per unit length and geometry, fully self-pinched Al and Mg plasmas were reproducibly formed near peak current. Copious x rays were emitted and detected. Figure 4 shows a typical current pulse and corresponding x-ray pulses detected by XRD's and PCD's in configuration A. The pulse widths
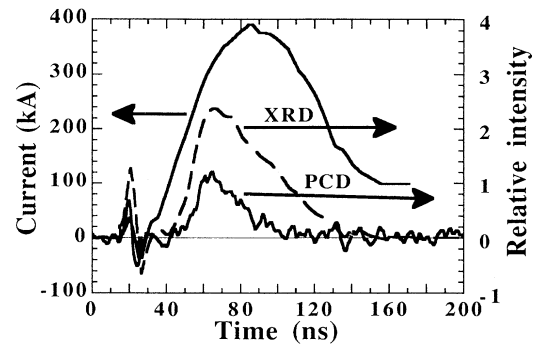

FIG. 4. Typical implosion current pulse and the corresponding x-ray pulses detected by filtered XRD's and PCD's with load configuration A.

of the x-ray signals fell in the range 20–40 ns (FWHM).

In configurations A and B, Mg L-shell spectra were obtained by viewing a region 1 cm long along the Mg plasma axis and 0.1 cm wide (in the radial direction) through the 40-μm entrance slit of the spectrometer, which was oriented parallel to the Mg plasma. The spectra were recorded on Kodak 101 films, which were read with a digitizing densitometer. Figures 5(a) and 5(b) show Mg spectra obtained with configurations A and B, respectively. Figure 5(c) shows the Mg spectrum from a pulse in which the Al wires in configuration A were replaced with a Mg wire. It should be noted that the spectra are time integrated, while the Al pump line radiation was emitted for at most a few tens of ns.

The presence of fluorescence in the Mg plasmas at 48.340 Å induced by the Al pumps was inferred by comparing the line intensity ratio R of the $2s4p$-$2s^2$ transition at 48.340 Å and the $2s^2\,{}^1S$-$2s3p\,{}^1P°$ transition at 62.75 Å in the three Mg spectra [Figs. 5(a), 5(b), and 5(c)]. We use the 62.75-Å Mg IX line for comparison, rather than other, more prominent Mg IX lines, as its intensity is a measure of the collisional excitation of Mg IX states from the ground state. Figure 5(c) does not show any line emission at 48.340 Å, consistent with there being no Al pump line radiation available to excite Mg IX ions. However, in configurations A and B [Figs. 5(a) and 5(b)], the Mg IX line at 48.340 Å is clearly seen because of the excitation of Mg IX ions to the $n = 4$ level by the Al line radiation, and the intensity ratio R is nearly 1. When the Al plasma was replaced by a Mg plasma [Fig. 5(c)], the intensity at 48.340 Å was in the background noise while the line intensity at 62.75 Å remained approximately the same as with the Al pump plasma, i.e., $-R$ is much less than one. Since the 62.75-Å line has the same lower state as the 48.340-Å line, if the 48.340-Å line radiation were induced in Mg IX by more collisional excitation and/or broadband photoexcitation on pulses with an Al pump plasma, the 62.75-Å line should have been much more prominent also. As shown in Figs. 5(a), 5(b), and 5(c), this was not the case.

As the measured fluorescence in the Mg IX line is coincident in wavelength with the Al ions, the enhanced Mg line emission at 48.340 Å could have been due to there

being Al ions in the Mg plasma, or to scattering of Al emission off a material surface in the spectrograph line of sight. Separation of the Al and Mg plasmas during the implosion was examined from the time-integrated x-ray pinhole image and the spatially and temporally resolved visible-light streak images taken through a slit oriented perpendicular to the discharge axis. Figures 6(a) and 6(b) show x-ray pinhole images of the plasmas obtained in configurations A and B, respectively, and Fig. 7 shows a visible-light streak image of the plasmas in configuration A. As shown in Figs. 6 and 7, intense visible light and x

rays were emitted from the regions along the wires only and no emission was seen from the region between them. Separation in space of the two plasmas during the implosion was inferred.

In order to be sure that no Al radiation was reflected off material surfaces into the spectrograph, many spectra obtained in our experiments have been carefully ana-
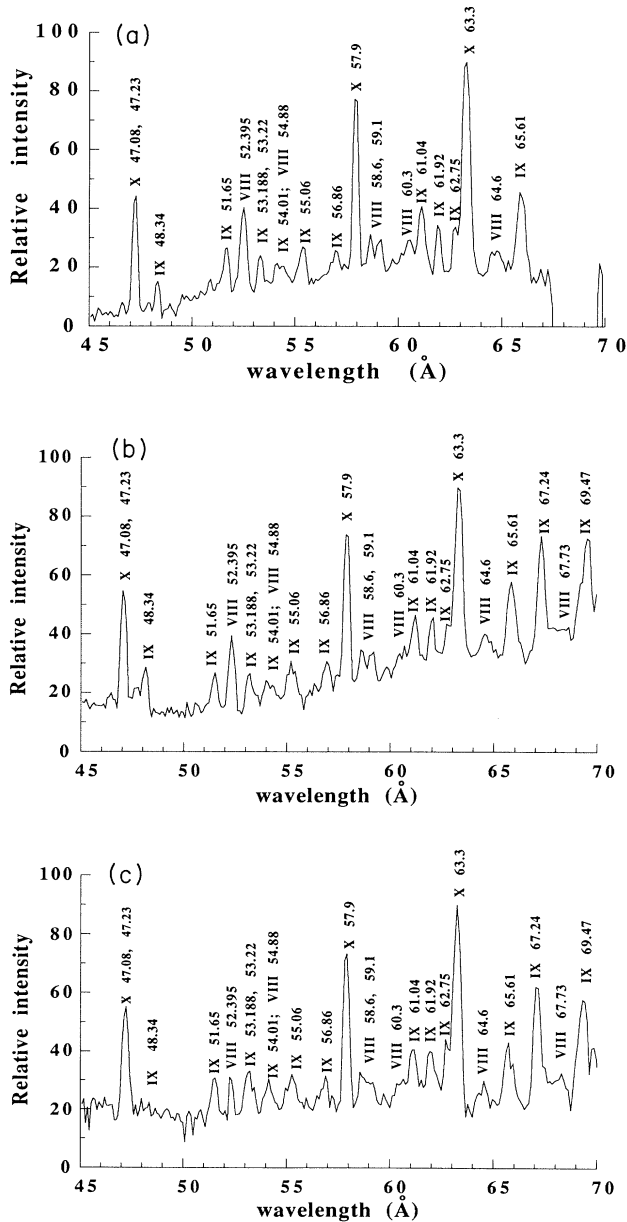

FIG. 5. Mg L-shell spectra obtained in configuration A and B are shown in (a) and (b), respectively. The Al plasma was replaced by a Mg plasma in configuration A to obtain the spectrum in (c).
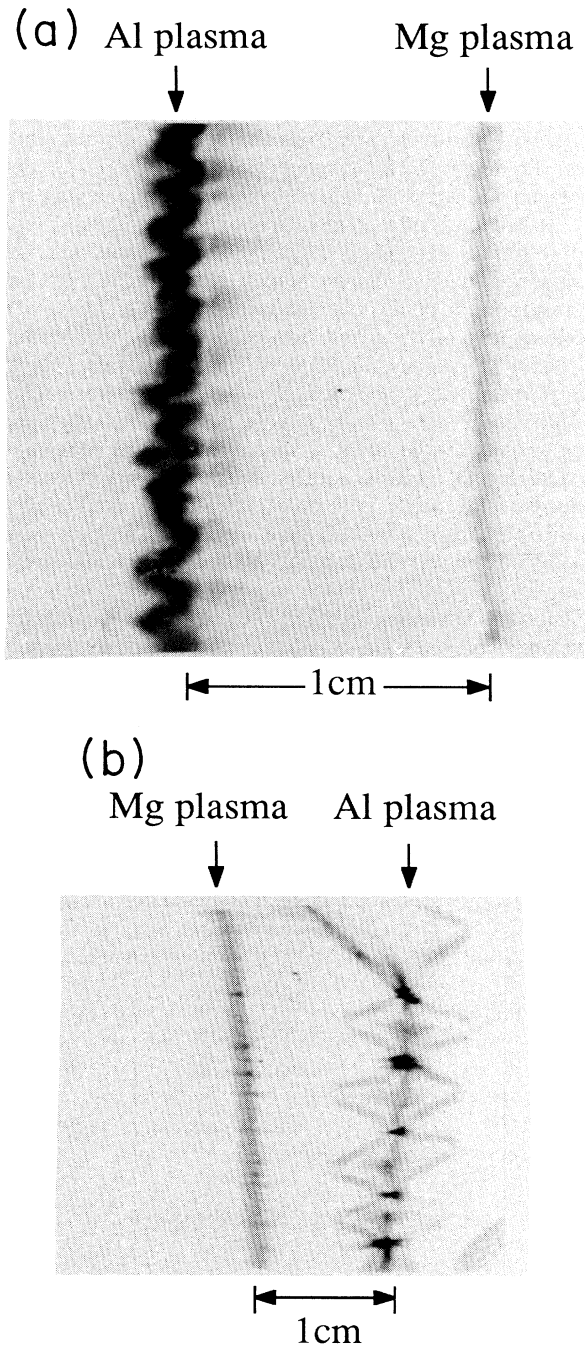

FIG. 6. Time-integrated x-ray pinhole images of the imploded plasmas in configurations A and B, respectively, are shown in (a) and (b). The radiation emission from the Mg plasmas in both cases was much weaker than the emission from the Al plasma.
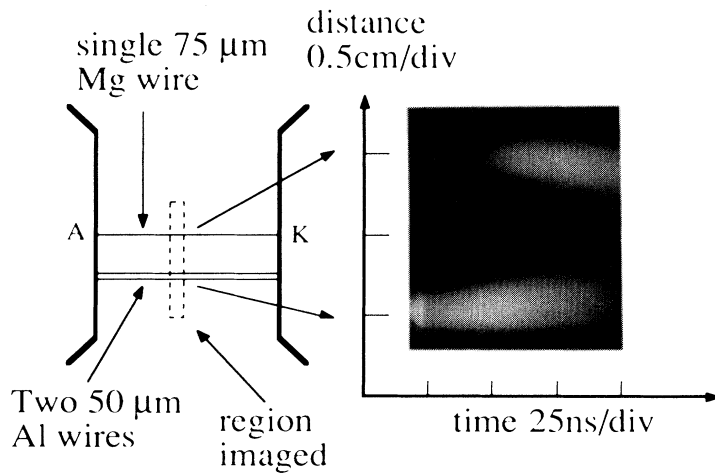
single 75 μm   distance
Mg wire   0.5cm/div

A   K

FIG. 7. Streak-camera image of the Al and Mg plasmas in configuration A.

Two 50 μm   region imaged
Al wires

time 25ns/div

lyzed. Figures 8(a) and 8(b) show higher-resolution Mg spectra obtained with configuration A in the wavelength regions between 46 and 58 Å, and between 56 and 68 Å, respectively, on a different test from that shown in Fig. 5(a). Figures 9(a) and 9(b) show the spectra with the Al wires in configuration A replaced by a Mg wire on a test other than that shown in Fig. 5(c). The spectra from an Al x-pinch plasma are shown in Figs. 10(a) and 10(b) for comparison. Intense resonant lines of Al XI at 48.338 and

52.446 Å, and Mg X lines at 57.920 and 63.152 Å are easy to identify and are used to determine the wavelengths of the other emission lines. These lines are then identified in Figs. 8–10 using published wavelengths [27]. The spectral resolution and the uncertainty in the wavelength calibration are both about 50 mÅ in the wavelength region between 46 and 68 Å. Intense line radiation from several Al ionization states, including emission from Li-like Al XI ions at 48.338 and 52.446 Å wavelength, and from Al X
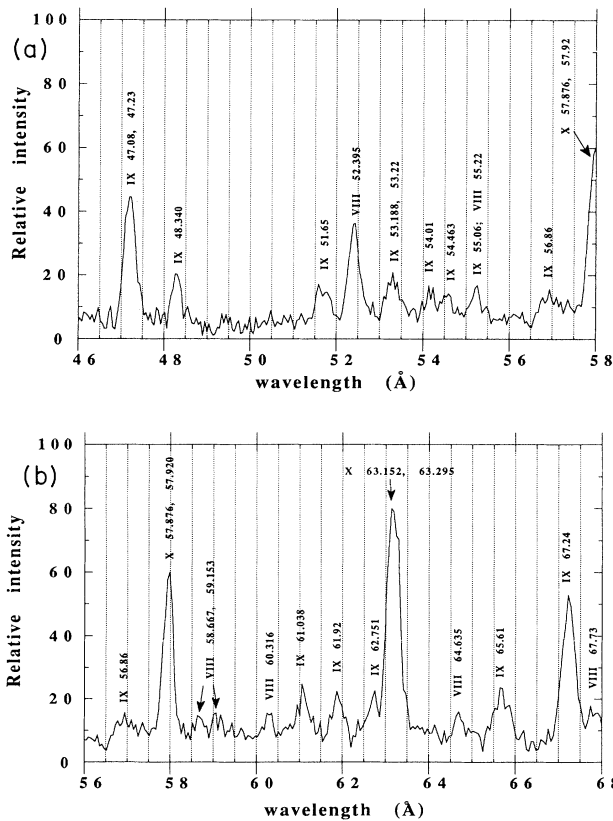

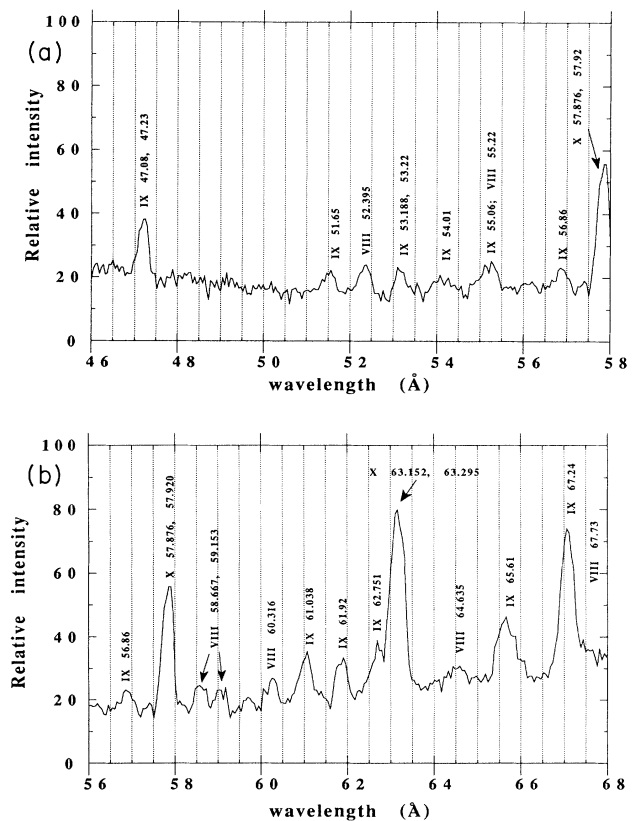FIG. 8. High-resolution Mg spectrum obtained with configuration A.

FIG. 9. High-resolution Mg spectrum obtained when the Al pump plasma in configuration A was replaced by a Mg plasma.
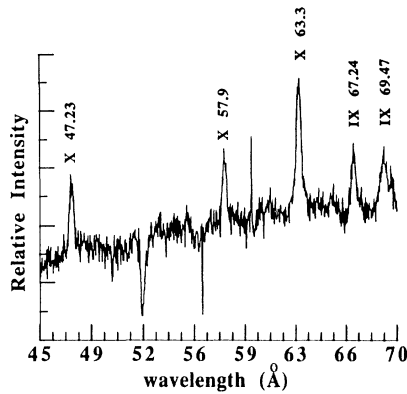
FIG. 10. High-resolution Al spectrum obtained from an Al x-pinch plasma.

they are not (see Figs. 8 and 9). Other strong Al lines at longer wavelengths than is shown in Fig. 10(b) were also not seen in the Mg spectra.

By contrast, when the initial separation between Al and Mg plasmas was reduced from 1.0 to 0.8 cm, the Mg and Al plasmas pinched toward each other. A typical visible-light streak image for such pulses is shown in Fig. 11 and the resulting Mg spectrum is shown in Fig. 12 for configuration A. The spectrometer was set to view the initial Mg wire position, which was 0.4 and 0.8 cm away from the pinched plasma axis and the initial Al wire positions, respectively. Since the bulk of the Mg plasma moved out of the spectrometer imaging region toward the Al plasmas, the recorded line emission was from the relative low temperature Mg ions before any motion occurred or from any Mg ions left behind during the pinch. As the result, the spectrum shown in Fig. 12 was about eight times weaker than that shown in Fig. 9. No emission at 48.34 Å was observed. It is possible that there were few Mg IX ions available to be photoexcited. Also, there are no Al lines observable in the spectrum. Therefore, we conclude that the observed emission at 48.340 Å was indeed due to the Mg IX line being photopumped by Al XI line radiation, and not from scattering off a material surface or Al impurity in the Mg plasma.

Clearly, it would have been much better to monitor radiation in the $n = 4$ to $n = 3$ transitions in Mg IX in order to demonstrate the successful photopumping. However, the sensitivity of our spectrometer in the range from 220 to 250 Å was inadequate to do this.

Fluorescence from the $2s2p^2 {}^4P - 2p^2({}^3P)4p\ {}^4D°$ transition at 52.395 Å in Mg VIII, pumped by the Al XI resonant line radiation at 52.446 Å may also have been observed. This is seen by comparing the line intensity at 52.395 Å with the line intensities for the other Mg VIII transitions. The ratio is smaller when the Al plasma is absent. The 51-mÅ wavelength mismatch between the 52.446 Å pump line and the 52.395 Å fluorescence line is about five times greater than the Doppler width of the Al pump line at a temperature of 150 eV. The wavelength mismatch could have been overcome by additional line broadening of the Al XI pump line due to photoreabsorption, Stark effect, and/or plasma stream motion [28].

ions at 55.376 and 57.02 Å, appears in the spectrum in Fig. 10(a). If the emission at 48.34 Å in the Mg spectra were due to scattering of the Al line by a material surface in our apparatus, or due to Al ions being in the Mg plasma, the lines from Al X at 55.376 and 57.02 Å as well as the several strong Al IX lines between 60 and 61 Å in Fig. 10(b), would have been detected on the Mg spectra, but

FIG. 11. Streak-camera image of the Al and Mg plasmas in configuration A with an initial separation distance of 0.8 cm. The Mg plasma was pinched toward the Al plasma.

FIG. 12. Mg L-shell spectrum obtained in the same pulse as for Fig. 11.

B. Estimated power in the pump transition

In configuration A, x-ray emission from the entire source region was detected by up to four calibrated PCD's filtered with 25-μm Be or 10-μm Al foil. These data were used to estimate the plasma densities and temperatures. As shown in the pinhole images [see Figs. 6(a) and 6(b)], radiation emission from the Al plasma was much more intense than that from the Mg plasma. With the wire mass per unit length and current per wire used in the present study, no K-shell line radiation from Al or Mg ions was observed with the KAP crystal spectrograph (which also viewed both Al and Mg plasmas). Furthermore, the L-shell line radiation energy was less than 400 eV (30 Å). Therefore, the radiation emission detected by the PCD's was apparently mainly from the free-free and free-bound transitions of the Li-like and/or Be-like Al XI ions. Using Eq. (5.3.54) in Ref. [29], intensity ratios of PCD signals yielded the plasma temperature, and the absolute signal intensities gave the electron density. The derived electron temperature was about 140 eV. Considering a 0.2-cm diameter Al plasma column measured from the x-ray pinhole image, the electron density of the Al plasma was about 10^{19} cm^{-3}.

The pump power of the Al XI $1s^2 2s\ ^2S_{1/2} - 1s^2 3p\ ^2P_{1/2}$ transition line at 48.338 Å in configuration A was estimated using the electron density, temperature, and plasma size quoted above and a simple two-level atomic model in which the upper $3p$ level was populated by electron collisional excitation [30] from the $2s$ ground state and depopulated by electron collisional deexcitation and radiative decay [31]. The rough-estimate result was about 10 MW, assuming 50% of the Al ions were in the Li-like ground state.

C. Magnesium plasma conditions

In configuration A, we also obtained rough estimates of the electron temperature and density in the Mg plasmas from experimental quantities. As line emission of Li-like Mg ions was observed, but there was no He-like Mg radiation, the electron temperature of the Mg plasma was in the range from 60 to 90 eV [32]. We estimated the size of

the Mg plasma from the pinhole image to be about 0.1 cm in diameter [see Figs. 6(a) and 6(b)]. From this, an electron density of about 10^{18} cm^{-3} from the intensity of the Mg X $1^2 2s\ ^2S_{1/2} - 1s^2 3p\ ^2P_{1/2}$ transition at 57.9 Å using the same method as we used to estimate the Al photopump power and assuming the emission pulse width was 10 ns.

To achieve useful gain in a Mg plasma, the electron density should be about 10^{18} cm^{-3}, and the electron temperature should be relatively low (≤ 40 eV) to greatly reduce deleterious collisional excitation from low-lying states to the lower laser level [28]. As very few Mg ions will be eight-times ionized at such a low temperature, photoionization of the Mg ions by Al plasma radiation is also crucial to achieving a high population inversion. In our experiments, the Mg plasma was produced within the desired density range. However, the Al plasma radiation power was too low to accomplish the broadband photoionization and resonant photoexcitation because of the relatively low driving current and the 1-cm separation distance between the two plasmas. We will discuss this issue later.

D. Results from configuration C

Fluorescence was also observed for load configuration C, in which the Al and Mg plasmas were produced in series. Figures 13–16 show the experimental data. Figure 13 shows the L-shell spectrum emitted from the Mg x-pinch plasma. As with configurations A and B, emission was observed for the Mg IX line at 48.340 Å, and the Mg VIII line at 52.395 Å. Figures 14(a) and 14(b) show the K-shell spectra from the Al and Mg x-pinch plasmas, respectively. Since the full pulse current was available to implode the three x pinches in series, all could reach the He-like and H-like ionization stages. Neither K-shell nor L-shell Al lines were found in the spectra from the Mg x-pinch plasma region other than the two lines noted above. Figure 15 shows the x-ray pinhole image of the multiple cross x-pinch plasma. Figure 16 shows the implosion current pulse, XRD signals obtained with 4-μm mylar and 1000-Å Al filters, and PCD signals filtered with 25-μm Be foil and with 10-μm Al foil. Bright xuv
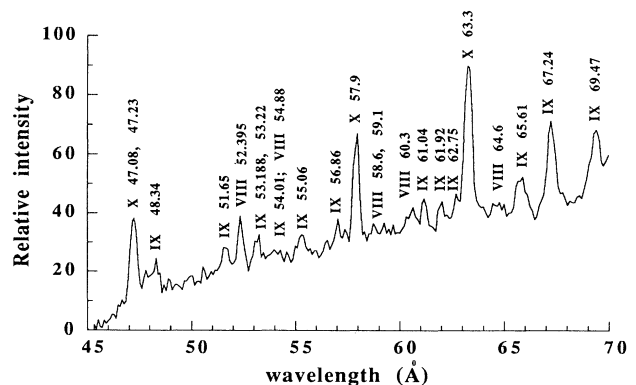

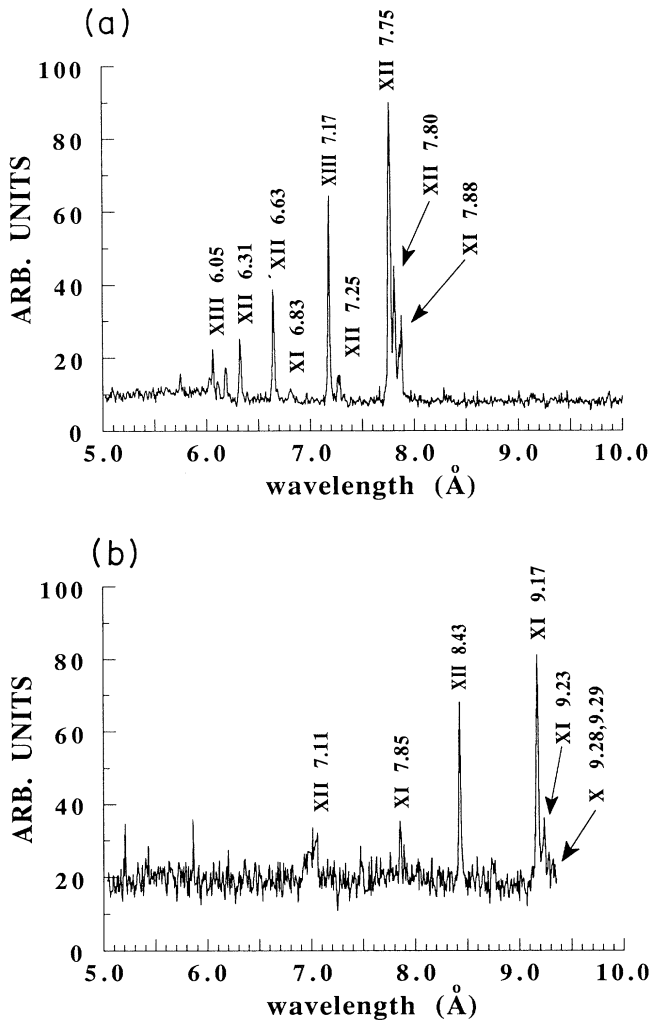
FIG. 13. Mg L shell spectrum obtained in configuration C.

FIG. 16. Typical implosion current pulse and the corresponding x-ray pulses detected by XRD's and PCD's in load configuration C. A Mg x-pinch plasma at cross point 2 was generated between two Al x-pinch plasmas at cross points 1 and 3 during the same pulse as for Fig. 15. Intense radiation is emitted from the regions where the wires were touching.

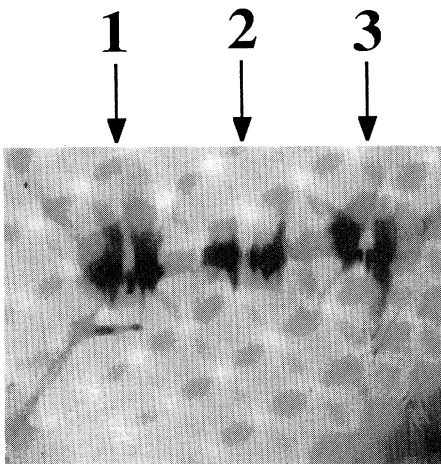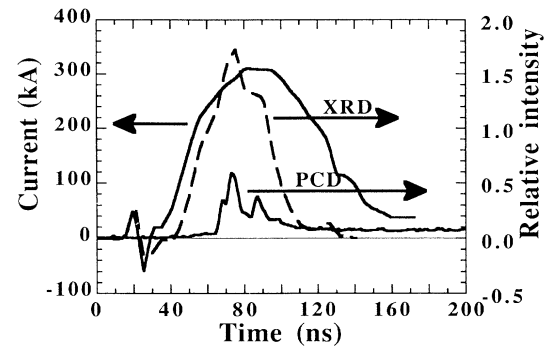FIG. 14. K-shell spectrum from an Al x-pinch plasma (a) and from the Mg x-pinch plasma (b) for configuration C.

FIG. 15. X-ray pinhole image of the multiple x-pinch plasma from configuration C.

and soft-x-ray (L- and K-shell) emission spots were observed at each cross point from the pinhole images. The typical size of these bright spots is about 2 mm in diameter. The K- and L-shell spectra were spatially resolved by putting a perpendicular slit in front of the spectrographs. Intense L-shell and K-shell line radiation was emitted from the wire crossing points only. In the regions between crossing points, no emission was detected in the K-shell spectra, while L-shell emission (along the wires) was much weaker than at the cross points. The spot size of the K-shell radiation was less than 100 μm, this limit being set by the spectrograph entrance slit. X-ray emission lasted for a few tens of ns. There were two intense x-ray pulses detected by the PCD's (see Fig. 16), while on the pinhole x-ray film there were seven x-ray spots distributed among the three cross points (see Fig. 15). Time coincidence of the emission from the individual cross point plasmas and, therefore,the moment of tightest pinching, is suggested.

The electron temperature and density in the pinch plasmas in configuration C were estimated independently by using line intensity ratios. Line emission from H-like and He-like ions was observed on the K-shell spectra [see Figs. 14(a) and 14(b)]. The line intensity ratio of the resonant $1s^2\,^1S_0 - 1s2p\,^1P_1$ transitions (Al XII 7.757 Å and Mg XI 9.1685 Å) and the intercombination $1s^2\,^1S_0 - 1s2p\,^3P_1$ transitions (Al XII 7.81 Å and Mg XI 9.23 Å) is strongly dependent on electron density, while the intensity ratio of the $1s2p^2\,^2D - 1s^22p\,^2P$ satellites (Al XI 7.87 Å and Mg X 9.294 Å) and the $1s^2\,^1S_0 - 1s2p\,^1P_1$ resonance lines depends on the electron temperature [33,34]. The estimated electron density and temperature for both Al and Mg plasmas were $\sim 10^{20}$ cm^{-3} and 220–270 eV, respectively.

E. Required pump power

In a photopump laser scheme, the most difficult task is to produce an intense radiation pump source. The required radiation power of the Al IX pump line is estimat-

ed as follows. Assuming a Doppler-broadened line profile, the gain coefficient G for a laser medium is given by

$$G = 1.6 \times 10^{-32} \lambda^3 A_{ul} \left[n_u - \frac{g_u}{g_l} n_l \right] \left[\frac{M}{T_e} \right]^{0.5} \text{cm}^{-1}, \quad (1)$$

where λ is the lasing wavelength in Å; n_u (or n_l) and g_u (or g_l) are the upper (or lower) lasing level populations in cm^{-3} and the statistic weight of the upper (or lower) population levels, respectively; A_{ul} is the spontaneous transition probability; T_e is the electron temperature of the laser medium in eV; and M is the atomic mass number. For a cylindrical geometry lasing medium with radius r and length l, the laser output power is given by

$$P_{\text{laser power}} = \pi r^2 l \, n_u \, A_{ul} \frac{hc}{\lambda}. \quad (2)$$

For a separation distance R between the two plasmas, the photopumping power is

$$P_{\text{pump power}} = P_{\text{laser power}} / \alpha, \quad (3)$$

where $\alpha (= \eta_\Omega \eta_\lambda \eta_p \eta_f \eta_r)$ is the pumping efficiency, including the solid angle subtended by the laser medium $(\eta_\Omega = rl/2\pi R^2)$; the wavelength mismatch between the pump line and the absorption line $(\eta_\lambda = 0.5)$; the fraction of the pump photons absorbed by the Mg IX ions $(\eta_p = 0.5)$; the fraction of the pumped electrons deexcited through the lasing channel $(\eta_f = 0.2)$; and the ratio of the pump photon wavelength to the lasing photon wavelength $(\eta_r = 0.2)$. From Eqs. (1)–(3) and ignoring absorption, we have

$$P_{\text{pump power}} = 2.4 \times 10^{20} \lambda^{-4} \left[\frac{T_e}{M} \right]^{0.5} r R^2 G \ \text{W}. \quad (4)$$

for a 228-Å wavelength laser with $r = 0.1$ cm, $R = 1$ cm, $T_e = 20$ eV, $M = 24$, and $G = 1$ cm^{-1}, the required pump power is on the order of 10 GW. Using a simple two-level coronal model, such power can be achieved in a Al plasma with an electron density of 10^{21} cm^{-3}, electron temperature of 200 eV, and plasma volume of 60 mm^3. These are consistent with the results from a detailed collisional-radiative model presented in Ref. [28].

In x-pinch experiments, up to 10-GW radiation power has been produced in Al K-shell radiation [35]. Softening the spectrum by cooling the Al pinch plasmas while maintaining or increasing the radiation pump power may be possible.

F. Proposed configuration for achieving population inversion

The most important disadvantage of the experimental configurations just presented is that the Al and Mg plasmas had to be 1 cm (or more) apart to avoid distortion of the Mg z pinch by the Al plasma except for the series configuration, which is unsuitable for pumping a laser. This disadvantage might be alleviated by symmetrizing the configuration, for example, with multiple cross Al x pinches on opposite sides of the Mg plasma. The ultimate symmetrization is a double coaxial z-pinch

configuration with an annular radiating Al plasma and a Mg plasma on axis.

Specifically, an extremely efficient pump geometry compared to the x pinch would result if an annular Al plasma could be imploded onto the Mg plasma without the two of them mixing, since they must remain separate for resonant photopumping. Inclusion of an initial axial magnetic field of about 1 T, and compressing it to ~ 100 T as a result of imploding the Al plasma, as illustrated in Fig. 17, could bring about this "ideal" situation. Such a large field would be expected to stabilize the Mg plasma on axis [36], which certainly appears unstable in Figs. 6(a) and 6(b), and to slow the growth rate of Rayleigh-Taylor instabilities on the inner surface of the Al plasma [37], in addition to isolating the two plasmas from each other. Recently, experiments with this double coaxial z-pinch configuration have been carried out for fusion studies [38]. Stabilizing of the core plamsa has been observed. Computer simulation of Al-Mg coaxial double pinch plasmas in the configuration illustrated in Fig. 17 shows that a gain of $1 - 1.5$ cm^{-1} is obtainable with an 800-kA current driver [39].

IV. CONCLUSIONS

In conclusion, we have achieved fluorescence in Mg IX emission by photopumping a Mg plasma with line emission from nearby Al XI plasmas as a first step toward achieving an xuv laser on the $2s4p$-$2s3d$ transition at 241 Å and/or on the $2s4f$-$2s3d$ transition at 228 Å of Mg IX. The $2s4f$-$2s3d$ transition may be the best candidate as it has a much larger oscillator strength [28]. We also have measured and/or estimated both Al and Mg plasma densities and temperatures.

However, the configurations tested in this work are unsuitable for the achievement of stimulated emission over a significant gain length. Both the proportion of the pump radiation intercepted by the laser medi⸱⸱m plasma and the laser medium conditions (density profile, temperature, and axial uniformity) are unacceptable. As a result, we are studying the configuration illustrated in Fig.
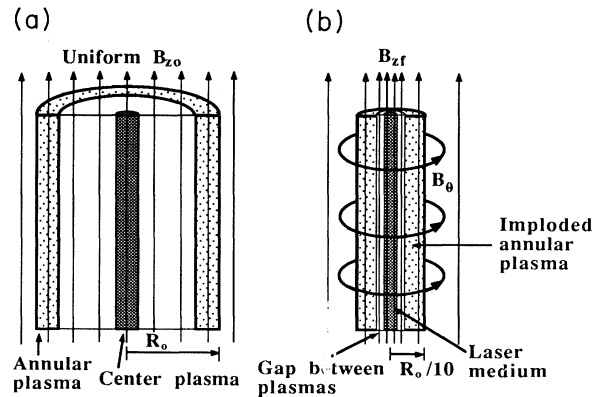

FIG. 17. Schematic diagram of our proposed xuv laser configuration, showing both the initial configuration (a) and the final configuration (b).

17 and briefly described in the last paragraph for the suit-ability of its final state as a possible effective xuv laser sys-tem. We believe that this configuration can be produced (including achieving the necessary final Al plasma condi-tions, i.e., $n_e \sim 5 \times 10^{19}$ cm^{-3}, $T_e \sim 150$ eV) with a ≤ 1 MA pulsed power generator. The initial Al and Mg plas-mas can be produced by injecting a high Mach number annular metal vapor plasma source [40] and a 10^{15} cm^{-3} discharge plasma, respectively, along the initial ~ 1-T magnetic field. Radial implosion of the Al plasma by a factor of 10 generates the ~ 100-T magnetic field men-tioned in the last paragraph, which should stabilize the Mg plasma with $n_e \leq 10^{18}$ cm^{-3} and $T_e \sim 30$ eV; it also produces an excellent pump geometry, as the two plas-mas will be very closely coupled.

*Present address: Science Research Laboratories, 1150 Ballena Blvd., Alameda, CA 94501.

[1] See, for example, J. Trebes, J. Phys. (Paris) Colloq. 47, C6-309 (1986); in *Applications of X-ray Lasers; Proceedings of the Workshop,* edited by R. A. London, D. L. Matthews, and S. Suckewer (NTIS, Springfield, VA, 1992).

[2] D. L. Matthews, P. L. Hagelstein, M. D. Rosen, M. J. Eckart, N. M. Ceglie, A. U. Hazi, H. Medecki, B. J. MacGowan, J. E. Trebes, B. L. Whitten, E. M. Campbell, C. W. Hatcher, A. M. Hawryluk, R. L. Kauffman, L. D. Pleasance, G. Rambach, J. H. Scofield, G. Stone, and T. A. Weaver, Phys. Rev. Lett. 54, 110 (1985); M. D. Rosen, P. L. Hagelstein, D. L. Matthews, E. M. Campbell, A. U. Hazi, B. L. Whitten, B. MacGowan, R. E. Turner, and R. W. Lee, *ibid.* 54, 106 (1985); J. B. MacGowan, S. Maxon, P. L. Hagelstein, C. J. Keane, R. A. London, D. L. Matthews, M. D. Rosen, J. H. Scofield, and D. A. Whelan, *ibid.* 59, 2157 (1987).

[3] S. Suckewer, C. H. Skinner, H. Milchberg, C. Keane, and D. Voorhees, Phys. Rev. Lett. 55, 1753 (1985).

[4] K. J. Ilcisin, U. Feldman, J. L. Schwob, A. Wouters, and S. Suckewer, J. Appl. Phys. 68, 5422 (1990); K. J. Ilcisin, Ph.D. dissertation, Princeton University, 1991.

[5] P. L. Hagelstein, Proc. SPIE 1551, 254 (1992).

[6] D. Kim, C. H. Skinner, G. Umesh, and S. Suckewer, Opt. Lett. 14, 665 (1989); J. Opt. Soc. Am. B 7, 2042 (1990).

[7] J. P. Apruzese and J. Davis, in *Proceedings of the Interna-tional Conference on Lasers, New Orleans, 1989,* edited by D. G. Harris and T. M. Shea (STS, McLean, VA, 1990), p. 7.

[8] M. C. Marconi and J. Rocca, Appl. Phys. Lett. 54, 2180 (1989); J. J. Rocca, M. C. Szapiro, and J. Meyer, Proc. SPIE 1551, 275 (1992).

[9] C. Steden and H. J. Kunze, Phys. Lett. A 15, 534 1990.

[10] A. V. Vinogradov, I. I. Sobelman, and E. A. Yukov, Kvant. Elektron. (Moscow) 2, 105 (1975) [Sov. J. Quantum Electron. 5, 59 (1975)].

[11] P. L. Hagelstein, Lawrence Livermore National Laborato-ry Report No. UCRL-53100, 1981 (unpublished).

[12] J. P. Apruzese, J. Davis, and K. G. Whitney, J. Appl. Phys. 53, 4020 (1982).

[13] J. P. Apruzese and J. Davis, Phys. Rev. A 31, 2976 (1985).

[14] S. J. Stephanakis, J. P. Apruzese, P. G. Burkhalter, G. Cooperstein, J. Davis, D. D. Hinshelwood, G. Mehlman, D. Mosher, P. F. Ottinger, V. E. Scherrer, J. W. Thornhill, B. L. Welch, and F. C. Young, IEEE Trans.

Plasma Sci. 16, 472 (1988).

[15] J. P. Apruzese, R. W. Clark, J. Davis, J. L. Porter, R. B. Spielman, M. K. Matzen, S. F. Lopez, J. S. McGurn, L. E. Ruggles, M. Vargas, D. K. Derzon, T. W. Hussey, and E. J. McGuire, in *Proceedings of 2nd International Colloqui-um on X-ray Lasers,* edited by G. J. Tallents (IOP, Bristol, 1991), p. 39.

[16] C. Deeney, T. Nash, R. R. Prasad, and J. P. Apruzese, Appl. Phys. Lett. 58, 1021 (1989).

[17] F. C. Young, V. E. Scherrer, S. J. Stephanakis, D. D. Hinshelwood, P. J. Goodrich, G. Mehlman, D. A. New-man, and B. L. Welch, in *Proceedings of the Interanational Conference on LASERS, Lake Tahoe, NV, 1988,* edited by R. C. Sze and F. J. Duarte (STS, McLean, VA, 1989), p. 98.

[18] J. L. Porter, R. B. Spielman, M. K. Matzen, E. J. McGuire, L. E. Ruggles, M. F. Vargas, J. P. Apruzese, R. W. Clark, and J. Davis, Phys. Rev. Lett. 68, 796 (1992).

[19] T. Boehly, M. Russotto, R. S. Craxton, R. Epstein, B. Yaakobi, L. B. Da Silva, J. Nilsen, E. A. Chandler, D. J. Fields, B. J. MacGowan, D. L. Matthews, J. H. Scofield, and G. Shimkaveg, Phys. Rev. A 42, 6962 (1990).

[20] M. Krishnan and J. Trebes, Appl. Phys. Lett. 45, 189 (1984).

[21] N. Qi and M. Krishnan, Phys. Rev. A 39, 4651 (1989).

[22] J. Maenchen, H. T. Sheldon, G. D. Rondeau, J. B. Green-ly, and D. A. Hammer, Rev. Sci. Instrum. 55, 1931 (1984).

[23] N. R. Pereira and J. Davis, J. Appl. Phys. 64, R1 (1988).

[24] N. Qi, D. A. Hammer, D. H. Kalantar, G. D. Rondeau, J. B. Workman, M. C. Richardson, and H. Chen, in *Dense Z-pinches,* edited by N. R. Pereira, J. Davis, and N. Ros-toker (American Institute of Physics, New York, 1989), p. 71.

[25] P. G. Burkhalter, D. B. Brown, and M. Gersten, J. Appl. Phys. 52, 4379 (1981).

[26] R. B. Spielman, W. W. Hsing, and D. L. Hanson, Rev. Sci. Instrum. 59, 1804 (1988).

[27] R. L. Kelly, J. Phys. Chem. Data 16, Suppl. 1 (1987).

[28] J. P. Apruzese and M. Buie, J. Appl. Phys. 70, 1957 (1991).

[29] I. H. Hutchinson, *Principles of Plasma Diagnostics* (Cam-bridge University Press, Cambridge, England, 1987), p. 175.

[30] M. J. Seaton, in *Atomic and Molecular Processes,* edited by D. R. Bates (Academic, New York, 1962), p. 374.

[31] W. L. Wiese, M. W. Smith, and B. M. Glennon, *Atomic Transition Probabilities,* Natl. Bur. Stand. Ref. Data Ser.,

Natl. Bur. Stand (U.S.) Circ. No. 4 (U.S. GPO, Washington, D.C., 1966), Vol. 1.

[32] M. Arnaud and R. Rothenflug, Astron. Astrophys. Suppl. Ser. **60**, 425 (1985).

[33] E. V. Aglitskii, V. A. Boilo, A. V. Vinogradov, and E. A. Yukov, Kvant. Elektron. (Moscow) **1**, 579 (1974) [Sov. J. Quant. Electron. **4**, 322 (1974)].

[34] J. P. Apruzese, D. Duston, and J. Davis, J. Quant. Spectrosc. Radiat. Transfer **36**, 339 (1986).

[35] D. A. Hammer, D. H. Kalantar, K. C. Mittal, and N. Qi, Appl. Phys. Lett. **57**, 2083 (1990).

[36] D. J. Rose and M. Clark, Jr., *Plasmas and Controlled Fusion* (MIT, Cambridge, MA, 1965), Chap. 14.

[37] A. B. Bud'ko, M. A. Liberman, A. L. Velikovich, and F. S. Felber, in *Dense Z-pinches,* edited by N. R. Pereira, J. Davis, and N. Rostoker (American Institute of Physics, New York, 1989), p. 272.

[38] H. U. Rahman, P. Ney, F. J. Wessel, A. Fisher, and N. Rostoker, in *Dense Z-pinches,* edited by N. R. Pereira, J. Davis, and N. Rostoker (American Institute of Physics, New York, 1989), p. 351.

[39] N. Qi, D. A. Hammer, and J. P. Apruzese (to be published).

[40] J. Ishikawa and T. Takagi, J. Appl. Phys. **56**, 3050 (1984).

single 75 μm
Mg wire

distance
0.5cm/div

A

K
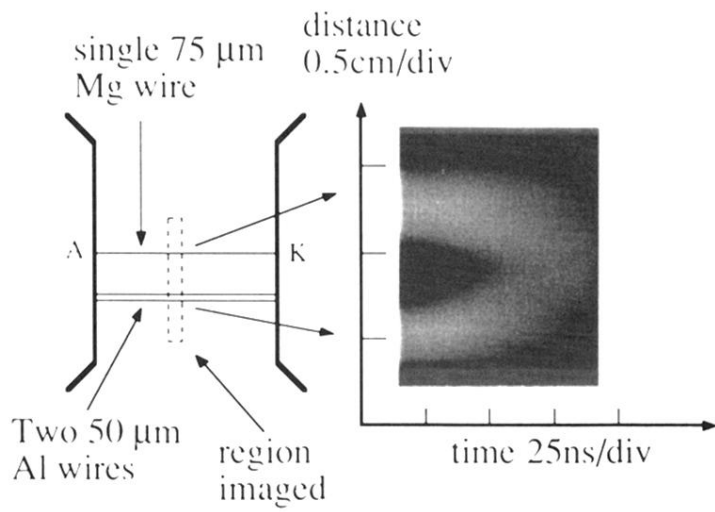
Two 50 μm
Al wires

region
imaged

time 25ns/div

FIG. 11. Streak-camera image of the Al and Mg plasmas in configuration A with an initial separation distance of 0.8 cm. The Mg plasma was pinched toward the Al plasma.
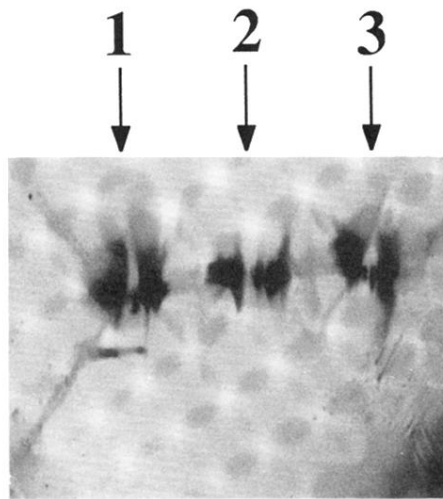
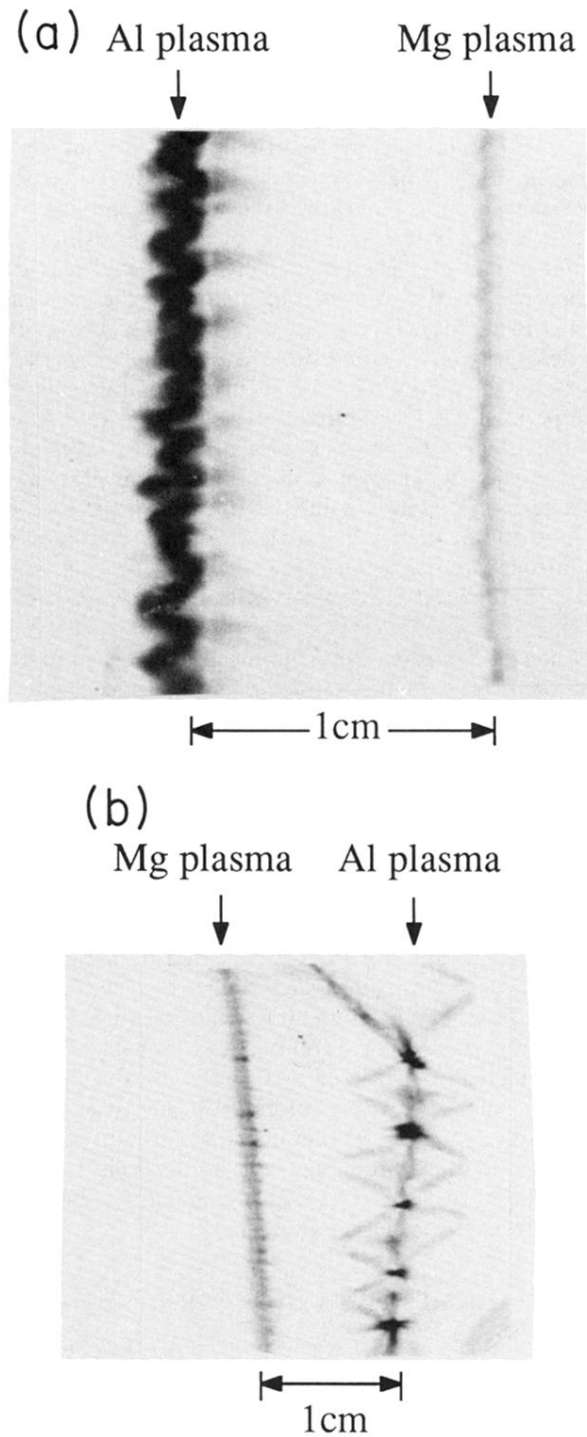FIG. 15. X-ray pinhole image of the multiple x-pinch plasma from configuration C.

FIG. 6. Time-integrated x-ray pinhole images of the implod-
ed plasmas in configurations A and B, respectively, are shown in
(a) and (b). The radiation emission from the Mg plasmas in both
cases was much weaker than the emission from the Al plasma.

single 75 μm
Mg wire

distance
0.5cm/div
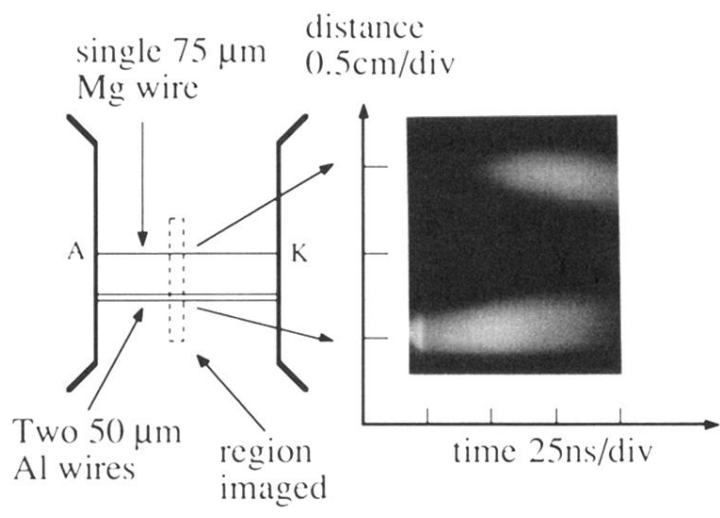
A

K

Two 50 μm
Al wires

region
imaged

time 25ns/div

FIG. 7. Streak-camera image of the Al and Mg plasmas in configuration A.